**Atmospheric
Chemistry
and Physics
Discussions**

The HNO$_3$ forming branch of the HO$_2$ + NO reaction: pre-industrial-to-present trends in atmospheric species and radiative forcings

O. A. Søvde[1,3]**, C. R. Hoyle**[2,3]**, G. Myhre**[1]**, and I. S. A. Isaksen**[1,3]

[1]Center for International Climate and Environmental Research – Oslo (CICERO), Norway
[2]Institute for Atmospheric and Climate Science, ETH Zurich, Zurich, Switzerland
[3]Department of Geosciences, University of Oslo, Norway

Correspondence to: O. A. Søvde (asovde@cicero.uio.no)

ACPD

11, 14801–14835, 2011

HO$_2$ + NO → HNO$_3$

O. A. Søvde et al.

Title Page

Abstract	Introduction
Conclusions	References
Tables	Figures

|◄ | ►|

◄ | ►

Back | Close

Full Screen / Esc

Printer-friendly Version

Interactive Discussion

Abstract

Recent laboratory measurements have shown the existence of a HNO_3 forming branch of the $HO_2 + NO$ reaction. This reaction is the main source of atmospheric O_3, through the subsequent photolysis of NO_2, as well as being a major source of OH. The branching of the reaction to HNO_3 reduces the formation of these species significantly, affecting O_3 abundances, climate and the oxidation capacity of the troposphere. The Oslo CTM2, a three-dimensional chemistry transport model, is used to calculate atmospheric composition and trends with and without the new reaction branch. Results for the present day atmosphere, when both temperature and pressure effects on the branching ratio are accounted for, show an increase of the global, annual mean methane lifetime by 10.9 %, resulting from a 14.1 % reduction in the global, annual mean OH concentration. Comparisons with measurements show that including the new branch improves the modelled O_3, but that it is not possible to conclude whether the NO_y distribution improves. We model an approximately 11 % reduction in the tropical tropospheric O_3 increase since pre-industrial times, as well as an 8 % decrease in the trend of OH concentration, when the new branch is accounted for. The radiative forcing due to changes in O_3 over the industrial era was calculated as $0.33 \, W \, m^{-2}$, reducing to $0.26 \, W \, m^{-2}$ with the new reaction branch. These results are significant, and it is important that this reaction branching is confirmed by other laboratory groups.

1 Introduction

Photochemical activity in the troposphere and lower stratosphere is strongly affected by the reaction

$$HO_2 + NO \rightarrow NO_2 + OH \tag{1}$$

which is the major source of O_3, through photodissociation of NO_2, and a major source of OH through recycling of HO_2. Changes in the concentration of OH lead to changes

in methane lifetime, and the resulting change in methane concentration then amplifies the change in OH concentration, in a "feed-back cycle".

Tropospheric O_3 has increased significantly since pre-industrial times, mainly due to increased emissions of NO_x (i.e. $NO + NO_2$), CH_4, CO and non-methane hydrocarbons (NMHC) (IPCC, 2001). Both in situ O_3 production and transport from e.g. the surface play important roles, especially for upper tropopsheric O_3. E.g. Berntsen et al. (1997) found a $\sim 35\%$ reduction in the tropospheric lifetime of O_3, due to enhanced HO_2 levels, while Lamarque et al. (2005) found a reduction of $\sim 30\%$. Hauglustaine and Brasseur (2001) found increases of surface O_3 over industrialised areas in the northern midlatitudes by more than a factor of 3.

Tropospheric OH is also affected by anthropogenic emissions: Increases in NO_x and O_3 (via NO_x) enhance OH, while increased levels of methane, CO, and hydrocarbons reduce OH levels. Model studies by e.g., Hauglustaine and Brasseur (2001); Shindell et al. (2003); Wong et al. (2004); Gauss et al. (2006) find a decrease in tropospheric OH levels since pre-industrial times, of maximum 33 %, although other studies also find a non-decrease of OH (IPCC AR4, 2007).

New information on the efficiency of Eq. (1) will therefore not only have consequences for modelled distributions of O_3, OH, and for the lifetime of methane, but will also influence the calculated trends in these species between pre-industrial times and the present.

Equation (1) is part of an efficient recycling of NO_x compounds, going through a large number of cycles before the NO_x is eventually converted to the less photochemically active species HNO_3, and removed from the atmosphere. The efficiency of Eq. (1) is highly dependent on altitude, latitude, and season.

The products of Eq. (1) were examined by Butkovskaya et al. (2005), who showed that a minor fraction goes through the branch that forms HNO_3:

$$HO_2 + NO \rightarrow HNO_3 \qquad (2)$$

Although they find that this branch only accounts for around 0.18–0.87 % of the products (at 298 K and 223 K, respectively), due to the large number of times NO_x is

$HO_2 + NO \rightarrow HNO_3$

O. A. Søvde et al.

recycled and passes through this reaction, the small branching ratio will still represent a significant loss. This pathway will therefore provide an important shortcut from NO to HNO_3, reducing the abundance of NO_2, and its contribution to O_3 and OH formation.

Beside the effect of temperature on the branching ratio, Butkovskaya et al. (2005) showed that the efficiency of the reaction increases in the presence of water vapour, more specifically by about 90 % at 3 Torr of H_2O. Their study was extended by Butkovskaya et al. (2007), presenting the branching ratio of the $HO_2 + NO$ reaction (in percent), as a function of air pressure (P, in Torr) and temperature (T, in Kelvin) below 298 K:

$$\beta(P,T) = (530 \pm 20)/T + (6.4 \pm 1.3) \times 10^{-4} P - (1.73 \pm 0.07) \qquad (3)$$

The effect of water on the branching ratio of Eq. (1) was not further investigated by Butkovskaya et al. (2007). Although to our knowledge these were the only experimental works which detected HNO_3 formation from Eq. (2), a reaction modelling study by Chen et al. (2009) also predicts HNO_3 formation, and at a similar rate to that found by Butkovskaya et al. (2007).

The effects of Eq. (2) on tropospheric and stratospheric chemistry were assessed by Cariolle et al. (2008), using a three dimensional tropospheric chemistry transport model (CTM) and a two dimensional stratosphere/troposphere CTM. They find substantial influence of the new reaction branch on tropospheric chemistry, including a 13 % mean global reduction in OH, a 5 % increase in methane lifetime and a 5–12 % decrease in tropospheric O_3. However, no radiative effects were calculated, and as only present day runs were performed, the effect on O_3 trends could not be investigated.

In the past, it has been shown that the Oslo CTM2, the model used in this study, has a high bias in O_3 concentrations, in the upper tropical troposphere (Søvde et al., 2008). A new reaction pathway by which the chemical production of O_3 is reduced has the potential to improve this bias, providing further motivation for this study.

The main focus of this study is on the changes in NO_x, O_3, OH, and the tropospheric lifetime of methane (τ_{CH_4}), leading to changes in the calculated trends of these

species since pre-industrial times, and ultimately to changes in radiative forcing since pre-industrial times. In the next section, the Oslo CTM2 is described, and in Sect. 3 we discuss the effects of the new reaction branch on atmospheric composition. In Sect. 4 the model simulations are compared more closely to observations, whereas the radiative forcing estimates are discussed in Sect. 5. Section 6 provides a summary and conclusions.

2 The Oslo CTM2

The Oslo CTM2 is a three dimensional off-line chemistry transport model (Berntsen and Isaksen, 1997; Berglen et al., 2004; Isaksen et al., 2005; Søvde et al., 2008, 2011), which was run in T42 (approximately $2.8° \times 2.8°$) resolution for this study. Vertically, the model is divided into 60 layers between the surface and 0.1 hPa. The meteorological data used is from 3 h forecasts generated by running the Integrated Forecast System (IFS) of the European Centre for Medium Range Weather Forecasts (ECMWF), for the year 2000. Meteorological data is updated (off-line) in the CTM every 3 h, however the transport time step is determined by the Courant-Friedrichs-Lewy (CFL) criteria, with a basic operator splitting time step of 1 h. The advection of chemical species is calculated by the second-order moment method, which is able to maintain large gradients in the distribution of species (Prather, 1986). Convective transport of tracers is based on the convective upward flux from the ECMWF model, allowing for entrainment or detrainment of tracers depending on the changes in the upward flux. Turbulent mixing in the boundary layer is treated according to the Holtslag K-profile scheme (Holtslag et al., 1990). In both convective and large scale precipitation, soluble species are dissolved in available cloud water according to their solubility (Henry's law or mass limited), and transported downward, where they can evaporate or ultimately be removed at the surface.

In the configuration used here the model chemistry accounts for the most important parts of the O_3-NO_x-hydrocarbon chemistry cycle in the troposphere and

Title Page

Abstract | Introduction

Conclusions | References

Tables | Figures

◀ | ▶

◀ | ▶

Back | Close

Full Screen / Esc

Printer-friendly Version

Interactive Discussion

includes a comprehensive stratospheric chemistry scheme. Heterogeneous reactions on aerosol and polar stratospheric clouds (PSC) are accounted for, as is the removal of HNO_3 through sedimentation of the PSC particles. For the chemistry calculations, the quasi steady state approximation (QSSA) chemistry solver (Hesstvedt et al., 1978) is used.

NO_x emissions from lightning are coupled on-line to the convection in the model using the parameterisation proposed by Price and Rind (1993) as described by Berntsen and Isaksen (1999). Emissions of CFCs, HCFCs, N_2O and other species with long tropospheric lifetimes are approximated with a constant lower boundary condition, according to WMO (2007). A list of chemical species, comprehensive model description and validation of ability of the Oslo CTM2 to reproduce the observed O_3 distribution is provided by Søvde et al. (2008). They also show that the model represents both the spatial and temporal variations of O_3 in the upper troposphere well, although the concentration is overestimated by up to 30–50 %. As shown below, the inclusion of Eq. (2) improves this bias.

The model experiments performed are listed in Table 1, and in the text below these experiments with and without Eq. (2) are also refered to simply as R2 and REF, respectively, when the year is evident from the context. All runs used the meteorological data for the year 2000, so that the only differences between REF and R2 are related to the inclusion of the new rection branch.

For the year 2000 model runs, anthropogenic emissions on a $1° × 1°$ grid were taken from the data base developed during the EU project POET (Precursors of Ozone and their Effects in the Troposphere) (Olivier et al., 2003; Granier et al., 2005). The methane surface mixing ratio was set to 1790 ppbv in the Northern Hemisphere, and 1700 ppbv in the Southern Hemisphere. The sum of hydrogen ($H_2O + 2CH_4 + H_2$) was set to 6.97 ppmv in the stratosphere, used to calculate stratospheric H_2O. The upper boundary conditions for all stratospheric species were taken from a year 2000 run of the Oslo 2-D CTM, as were the surface mixing ratios for species with long tropospheric lifetimes (i.e. those which do not need to be explicitly included in the tropospheric chemistry

scheme), as in Søvde et al. (2008).

In the pre-industrial runs, all anthropogenic emissions were switched off; only the natural emissions for the year 2000 were used. The surface mixing ratio of methane was set to 791.6 ppbv, and the sum of stratospheric hydrogen was set to 5.08 ppmv.
Similarly as in the year 2000 run, the upper and lower boundary conditions of stratospherically relevant species were prescribed by model output from a pre-industrial run of the Oslo 2-D model.

3 Results

The immediate response of Eq. (2) is to reduce HO_2 available for NO_2 production by Eq. (1). There are also secondary effects occuring, and in this Section we present the effect of Eq. (2) on NO_2, HNO_3, O_3, CH_4, and OH, as well as changes in trends since pre-industrial times.

3.1 Effect of Eq. (2) on NO_2

The July and December zonal monthly mean NO_2 mixing ratios for REF_2000, in are shown in Fig. 1a,c, respectively. Corresponding percentage changes in NO_2 mixing ratio from REF_2000 to R2_2000 are shown in panels b and d. Mixing ratios in panels a and c are substantially higher in the stratosphere than the troposphere, and near the surface enhanced NO_2 values can be seen due to industrial emissions in the Northern Hemisphere. The lower values around 20 km over the Antarctic and Arctic, in July and December, respectively, are due to the formation of reservoir species such as HNO_3, which are relatively stable in the low light conditions.

In panels b and d, the greatest percentage reduction in NO_2 mixing ratio as a result of the new reaction branch occurs between about 10 km and 20 km altitude in the tropical to mid-latitude regions. This was also predicted by Cariolle et al. (2008), however the reduction calculated here is around twice as large. Smaller effects are seen throughout

the stratosphere. Below 10 km, there are also reductions of NO_2 of around 40% in July over the Arctic, and around 80 % in December over the Antarctic. However, due to the low NO_2 mixing ratios in these regions, the change is not really important. The $\sim 6\%$ increase in NO_2 at high northern latitudes in December also involves small NO_2 mixing ratios, and comes about because the reduced OH from Eq. (1) also leads to a reduction in the efficiency of the reaction

$$NO_2 + OH + M \rightarrow HNO_3 + M, \tag{4}$$

giving smaller NO_2 loss. In areas with more incident solar radiation this effect is not seen, due to higher OH abundances.

Because of the distribution of NO_2, the main effect of the new reaction branch is seen in the upper troposphere and lower stratosphere at low latitudes.

3.2 Effect of Eq. (2) on HNO_3

The July and December zonal monthly means of modelled HNO_3 are shown in Fig. 2a,c, respectively, showing well-known maximum values in the stratosphere. The low values over the Antarctic in July (panel a) are due to the sequestering of HNO_3 in PSC particles.

The inclusion of Eq. (2) leads to a direct increase in HNO_3 mixing ratio in some areas. However, the new reaction branch also changes other processes affecting HNO_3, making the effect of the reaction less intuitive.

OH produced from Eq. (1) is reduced due to Eq. (2), in turn reducing the rate of HNO_3 production via Eq. (4), giving a total reduction of HNO_3. The influence of this can be seen in the troposphere at high latitudes. When more tropospheric HNO_3 is formed from Eq. (1) in areas of wet deposition by rain, more HNO_3 will be rained out, reducing the availability of precursors for HNO_3 formation in other areas.

Percentage increases in HNO_3 are greatest in the tropics between 10 km and 20 km altitude, and in the stratosphere, above about 30 km (Fig. 2, panels b and d, respectively). In the Southern Hemisphere, in July, there is a reduction in HNO_3 of almost

$HO_2 + NO \rightarrow HNO_3$

O. A. Søvde et al.

Title Page

Abstract	Introduction
Conclusions	References
Tables	Figures

◄ | ►|

◄ | ►

Back | Close

Full Screen / Esc

Printer-friendly Version

Interactive Discussion

20 % near the surface in R2_2000 compared to REF_2000, while there is a small increase over the Arctic (panel b). In December, there is a 15–20 % increase in HNO_3 at around 5 km over the Antarctic (panel d). These changes at 5–10 km over the polar regions come about as the vertical HNO_3 gradient in this area is very high (see panels a and c), and in R2 the region of low HNO_3 is confined to slightly lower altitudes. The slight shift in the vertical position of the isolines creates a large percentage change. Also in December, the increase in HNO_3 above 10 km altitude in the tropics is paired with a decrease in HNO_3 of 10 % to 15 % at an altitude of ~ 20 km, again suggesting a vertical shifting of the HNO_3 distribution between the two runs, in addition to the extra HNO_3 production. This additional HNO_3 formed in the troposphere will be subject to wet deposition, reducing the amount of NO_x and HNO_3 transported to higher altitudes, hence the decrease at ~ 20 km.

3.3 The effect of Eq. (2) on OH and CH_4

The tropospheric, annual mean OH concentration was calculated for the four model runs, and the results are shown in Table 2. The mean OH concentration calculated in REF_2000 is slightly higher than the recent values listed in Wang et al. (2008), however a good agreement is reached when the new reaction branch is taken into account (R2_2000). The reduction in the mean OH concentration, caused by Eqs. (1) and (2), is about 13 % and 14 % for 1850 and 2000, respectively, similar to the approximately 13 % decrease calculated for the present day by Cariolle et al. (2008). From 1850 to 2000, the OH concentration declines by 12.1 % in the R2 cases, compared to 11.2 % in the REF cases.

The methane lifetime, being controlled predominantly by the concentration of OH, is around 10–11 % larger in the R2 cases than in the REF cases (Table 3). This is about twice the increase calculated by Cariolle et al. (2008) (ca. 5 %), however without performing a detailed model intercomparison, it is not possible to say what the cause of this difference is. The change in methane lifetime between REF_1850 and REF_2000 is 4.6 %, and the change between R2_1850 and R2_2000 is 4.0 %.

Taking the new reaction branch into account leads to a significant decrease in the OH concentration, but also a greater decline of OH since pre-industrial times, leading to a greater calculated anthropogenic impact on the oxidising capacity of the atmosphere, and therefore the lifetime of methane.

3.4 Effect of Eq. (2) on O_3

The difference between the the tropospheric zonal mean O_3 column for REF_2000 R2_2000 and is plotted as a function of time and latitude in Fig. 3. Equation (2) reduces this O_3 column everywhere, with a maximum reduction of -5.8 DU. The main effect of the new reaction branch is seen in the tropics, with the smallest effect at polar latitudes. A reduction of up to about -3.5 DU occurs at high northern latitudes in July to August, which can be explained by the greater summer-time photodissociation leading to a more rapid removal of NO_x through Eq. (2). At high southern latitudes there is also a seasonal dependence. The smallest effect is seen at high northern latitudes in winter.

The July and December zonal monthly means of modelled O_3 from R2_2000 is shown in Fig. 4 (panels a and c, respectively), with corresponding percentage changes between REF_2000 and R2_2000 shown in panels b and d.

The decrease in NO_2 production between REF_2000 and R2_2000 leads to a reduction in O_3 formation, and therefore up to about 14–16 % lower O_3 values, predominantly in the upper tropical troposphere, although the percentage change in Fig. 4 is large throughout the troposphere. Again, the amount of O_3 in the middle and lower troposphere is small, as shown in panels a and c. There is a reduction in O_3, in the lower troposphere, at high northern and southern latitudes (panels b and d, respectively). Although the percentage change in panel d reduction is very large, O_3 levels in this region are low, therefore this change has a very small effect on mean tropospheric O_3 values. The small increase in O_3 at high latitudes, at an altitude of around 25 km, is due to the reduction in NO_x induced O_3 loss.

3.5 Effect on trends of tropical O_3

Both in the pre-industrial runs and in the year 2000 runs, the O_3 mixing ratios were lower in R2 than in the REF case. The reduction is greater in the year 2000 runs, therefore the trend in O_3 mixing ratios since the pre-industrial times is also affected. In order to better quantify the effect on O_3 trends since the pre-industrial times, we have calculated the changes in mixing ratios within a section of the tropical troposphere, where the greatest influence of Eq. (2) was seen. This section extends between the approximate latitudes of $15°$ S to $15°$ N, and from approximately 5.5 km to 15 km in altitude.

Within this volume, the increase in O_3 between 1850 and 2000 for July was 52.7 % in the REF case, and 48.4 % in the R2 case, leading to a difference in O_3 increase of -8.1%. Averaged over the whole year, the change in O_3 trend is -11.1%.

4 Comparison with measurements

In Sect. 3 we have shown the effects of Eq. (2), and these effects must be evaluated against observations. We do this by comparing model results to satellite measurements as well as in-situ measurements. First we compare O_3, then nitrogen species.

4.1 Modelled and measured O_3

In order to confirm that the model represents the observed O_3 fields correctly, monthly averages of modelled total column O_3 (R2_2000) are plotted in Fig. 5, along with the average total column O_3 measured by the Total Ozone Mapping Spectrometer (TOMS), for January, April, July and October. For most months, and over most of the globe, the agreement between the modelled and the measured values is excellent. In January, the model overestimates the column O_3 west of Europe, and over the Antarctic, and slightly underestimates the values over the tropics, however the main features of the

column O_3 distribution are captured well. In April and July, there is very little difference between the modelled and measured columns, with slightly lower values in the model in the tropics and slightly higher values at mid-latitudes in the Southern Hemisphere, than in the TOMS data. In October, the column values to the west of Europe as well as over North America and Northern Africa are again slightly overestimated by the model, however, the magnitude and extent of the Antarctic O_3 hole is well represented.

We have produced modelled O_3 profiles at the time and location of all O_3-sondes at 11 stations within the framework of SHADOZ (Thompson et al., 2003). These stations are located predominantly in the tropics, where Eq. (2) has the largest effect, and are listed in Table 4, including the number of sondes through the year. Annual averages of measured and modelled O_3 profiles are shown in Fig. 6.

In the lower and middle troposphere, the SHADOZ sondes measure smaller O_3 mixing ratios than the model predicts, with REF_2000 overestimating the measured values by 16 ppbv, or almost 33 % at about 300 hPa. In R2_2000 however, this overestimation is reduced to only 7 ppbv, or 14 %. Above $\sim$ 200 hPa and in the lower troposphere (below $\sim$ 500 hPa), the R2_2000 O_3 mixing ratios are very similar to the measured values. The inclusion of Eq. (2) therefore leads to a significant improvement in the models ability to reproduce the observed tropospheric O_3 values.

4.2 Modelled and measured NO, NO_y and O_3

Tropical tropospheric O_3 production is largely controlled by the amount of nitrogen species. The amount of nitrogen species is mainly controlled by emissions from the surface and from lightning, combined with rainout of HNO_3, whereas chemistry and clouds are most important for the partitioning.

Comparing modelled NO, NO_2 and HNO_3 with measurements is challenging and should therefore be carried out with care. NO_2 is seldom measured, and the partitioning between NO and NO_2 depends on sunlight. Unless the modelled cloud cover very closely matches the cloud cover at the time and location of the measurement (a difficult task, given the sub-grid scale variability of clouds), such a comparison will be difficult,

Title Page

Abstract | Introduction

Conclusions | References

Tables | Figures

◄ | ►

◄ | ►

Back | Close

Full Screen / Esc

Printer-friendly Version

Interactive Discussion

since NO is usually measured only during day-time.

However, an important part of the nitrogen budget is HNO_3, which is washed out by rain. Precipitation and the associated wet scavenging of chemical species has a variability which cannot be resolved by large scale models, and this may hamper the comparison with measured HNO_3, as well as other nitrogen components.

Atmospheric measurements of upper tropospheric nitrogen species are rather limited; only a few aircraft campaigns are available. Instead of comparing the model to a climatology, we compare the model with in-situ measurements carried out by CARIBIC flights (Civil Aircraft for the Regular Investigation of the atmosphere Based on an Instrument Container, Brenninkmeijer et al., 2007, http://www.caribic-atmospheric.com). Measurements used in this comparison are O_3 (A. Zahn, personal communication) and NO and NO_y (H. Ziereis, G. Stratmann, H. Lichtenstern, H. Schlager and U. Shumann, personal communication, 2011). In order to do this for R2 and REF, simulations are carried out with meteorological data for the year 2005, a year with frequent CARIBIC flights in the tropics. Emissions data used in these simulations were for 2000 except biomass burning which was for 2005.

Atmospheric species are retrieved from the Oslo CTM2 at the time and location of all CARIBIC measurements (flights 110–136, only missing flight 137 due to technicalities), allowing a one-to-one comparison. In Fig. 7 we show time series of these species at the location and times where NO was measured, at the aircraft cruise altitude around 200 hPa. Only measurements above 400 hPa are used, to limit comparison to the free troposphere. A few observations are located in the stratosphere and are shown in blue in the figure. As was the case for the SHADOZ comparison, the comparison of modelled O_3 with the CARIBIC measurements (upper time series) is slightly better for R2. NO_y (lower time series) is close to unchanged by the inclusion of Eq. (2), while NO (middle) is slightly reduced. It is not, however, possible to conclude whether or not Eq. (2) improves the modelled NO. In both REF and R2, the model fails to catch high values of NO and NO_y, probably due to either unresolved variation in surface emissions, or the transport of emitted species to the free troposphere, unresolved variation

Discussion Paper | Discussion Paper | Discussion Paper | Discussion Paper | Discussion Paper |

[ACPD](#)

11, 14801–14835, 2011

$HO_2 + NO \rightarrow HNO_3$

O. A. Søvde et al.

Title Page

Abstract | Introduction

Conclusions | References

Tables | Figures

|◄ | ►|

◄ | ►

Back | Close

Full Screen / Esc

Printer-friendly Version

Interactive Discussion

CC BY

in lightning emissions of NO$_x$, or the limitations in modelling wet scavenging discussed above.

For these simulations HNO$_3$ above 100 hPa has also been compared profile-by-profile to measurements by the Earth Observing System Microwave Limb Sounder (MLS) aboard the AURA satellite, showing a slight improvement from REF to R2 (not shown). However, the effect on O$_3$, compared for the same satellite profiles, was negligible at these altitudes.

The study here and that of Cariolle et al. (2008) both show that Eq. (2) is most important at tropical altitudes between ~ 8 km and ~ 17 km. In contrast to the model results shown in their work, the Oslo CTM2 reproduces O$_3$ measurements well, also above 8–12 km, where the largest effect of the reaction is found. If O$_3$ is not well modelled in the region of interest, it is hard to reach a conclusion on whether or not NO$_x$ and HNO$_3$ are correctly represented. Cariolle et al. (2008) compared their model against a climatology of NO$_x$ and HNO$_3$ compiled from aircraft campaigns, and a climatology O$_3$ from sondes, and concluded without much discussion that Eq. (2) tended to make their model results worse.

From their figures (number 5 and 6), it seems that NO$_x$ is underestimated when including Eq. (2). If their NO$_x$ emissions had been higher, however, the NO$_x$ decrease associated with Eq. (2) would have lead to a better agreement with observations. More NO$_x$ would also increase tropospheric O$_3$. HNO$_3$ would also increase, however, since wet removal of HNO$_3$ is mass limited, it is difficult to predict how relevant the changes would be. It should be noted that the relative statement made by Cariolle et al. (2008), that the new reaction path leads to an overall worsening in the modelled results, is not applicable to all atmospheric models. Whether a model's results "improve" or "worsen" depends on whether it over or underestimated a particular species before addition of the new reaction branch. Far more important is the fact that both our study, and that of Cariolle et al. (2008) show that the new reaction branch leads to a net reduction in tropospheric O$_3$.

HO$_2$ + NO → HNO$_3$

O. A. Søvde et al.

Title Page

Abstract | Introduction

Conclusions | References

Tables | Figures

◄◄ | ►►

◄ | ►

Back | Close

Full Screen / Esc

Printer-friendly Version

Interactive Discussion

In fact, their lightning emissions were $4\,\mathrm{Tg\,(N)\,year^{-1}}$, whereas the Oslo CTM2 uses $5\,\mathrm{Tg\,(N)\,year^{-1}}$. Although both are within the range $5 \pm 3\,\mathrm{Tg\,(N)\,year^{-1}}$ presented by Shumann and Huntrieser (2007), lightning emissions are predominantly located in the upper tropical troposphere where Eq. (2) has a large impact, therefore their lower emis-
5   sions could very well explain the differing conclusions of their study.

There are also uncertainties in surface emissions, e.g. biomass burning and its ver-
tical distributions may differ from model to model. Surface NO_x emissions in the Oslo CTM2 amounts to $44\,\mathrm{Tg\,(N)\,year^{-1}}$, slightly higher than the $42\,\mathrm{Tg\,(N)\,year^{-1}}$ used by Cariolle et al. (2008). In addition there are uncertainties in meteorologies driving the
10 models, and treatment of convective transport will also be important in distributing these emissions. As noted, the wet scavenging will play an important role by removal of HNO_3, and slightly weak removal combined with slightly low emissions could pro-
duce reasonable amounts of atmospheric nitrogen species. From our results, and the results of Cariolle et al. (2008), we cannot conclude whether Eq. (2) makes the model
15 NO_x and NO_y results better or worse, only that the impact is important for O_3 and that the existence of the reaction needs to be confirmed by other measurements.

5   Radiative forcing

The changing emissions to the atmosphere since pre-industrial times lead to a change in the O_3 concentration and therefore a radiative forcing (RF). In this section we inves-
20 tigate the magnitude of this forcing and the influence of the new reaction branch. The RF was calculated using separate radiative transfer codes for long-wave and short-
wave radiation, in off-line simulations. A broad band code for long-wave (Myhre and Stordal, 1997) and a model using the discrete-ordinate method (Stamnes et al., 1988) for short-wave radiation were adopted. Meteorological data from the ECMWF was used
25 for simulations on a monthly mean time scale. A stratospheric temperature adjustment was included (Myhre et al., 2000), to follow the standard definition of radiative forcing (Forster et al., 2007).

In addition to the REF and R2 runs already described, two simulations with and without Eq. (2) for the year 2000 were performed with Cl and Br at 1850 levels, to separate out the effect of halogens. In Table 5 we show the radiative forcing from tropospheric O_3 precursors and Cl/Br. Values are given for the troposphere (upper), stratosphere (middle) and both (lower). The total RF due to emission changes since pre-industrial times is $0.33\,W\,m^{-2}$, which reduces to $0.26\,W\,m^{-2}$ in R2, due to the reduced growth in tropospheric O_3. The greatest contributions to the calculated RF were due to the tropospheric precursors such as NO_x, CH_4, CO and NMHC which also lead to an increase in the stratospheric O_3. Of the total of $0.52\,W\,m^{-2}$ from tropospheric O_3 precursors in the R2 simulations, changes in the stratosphere contributed $0.08\,W\,m^{-2}$.

Stratospheric changes resulting from Cl and Br increases amounts to $-0.20\,W\,m^{-2}$, giving RF due to stratospheric O_3 change of $-0.12\,W\,m^{-2}$. The reduction in stratospheric O_3 due to Cl and Br leads to less O_3 being transported from the stratosphere into the troposphere than if Cl and Br were absent. This causes a negative contribution to the tropospheric O_3 development since pre-industrial times, amounting to $-0.06\,W\,m^{-2}$ in the R2 simulations, hence giving a negative contribution to the RF in both the stratosphere and the troposphere.

In other words, the total RF influence of this halogen induced O_3 change in the troposphere and stratosphere is $-0.26\,W\,m^{-2}$, a number that is unchanged from REF to R2.

It should be noted that the stratospheric halogen chemistry can take place to slightly lower altitudes in the CTM than the tropopause used in the RF calculations. Therefore, some of the $-0.06\,W\,m^{-2}$ attributed to transport from the stratosphere could in fact be due to the direct influence of Cl and Br chemistry in the upper troposphere of the RF calculations.

The geographical distribution of the stratospheric and tropospheric RF components are shown in Fig. 8, panels a and b, respectively, for the R2 case. Relatively large tropospheric RF values are found between about 30° S and 60° N, where substantial industrial emissions occur. The greatest RF is found over Saudi Arabia, Northern Africa

and Iran, where the O_3 increase is coupled with high solar irradiance and high surface reflectivity, as well as temperature and cloud amount conditions for a high long-wave RF (Berntsen et al., 1997). The stratospheric RF is generally negative, due to halogen related O_3 loss since the pre-industrial times. Values are around zero at low latitudes, and the RF becomes more negative towards high latitudes, with the strongest values of $-1.1\,\mathrm{W\,m^{-2}}$ over Antarctica. The RF in the REF case is similarly distributed and differs only in magnitude, with only minor differences in the magnitude for O_3 changes in the stratosphere.

6   Summary and conclusions

A set of model runs was performed to evaluate the chemical and climate implications of the HNO_3 forming branch of the $HO_2 + NO$ reaction. We found that despite the small branching ratios, the atmospheric effects are important, especially in the upper tropical troposphere. NO_x concentrations decrease by up to $\sim 50\,\%$ in the troposphere, via conversion to HNO_3 and subsequent wet deposition of HNO_3, making the removal permanent in some regions.

The reduction in NO_x leads to a reduction in the formation rate of O_3, reaching $\sim 18\,\%$ in the tropical upper troposphere in December. The reduction in tropospheric O_3 is greatest in the tropics (up to $5.8\,\mathrm{DU}$), and is the least at high latitudes. The annual, global mean OH concentration decreases by 14.1 %, and as a result the methane lifetime increases by 10.9 %.

The increase in tropospheric O_3 since pre-industrial times is reduced by the inclusion of the new reaction branch, with tropical tropospheric O_3 increasing by an annual average of 11 %. Our model shows that OH has decreased since pre-industrial times, and the new reaction branch reduces this decrease. This means that the calculated increase in CH_4 lifetime since 1850 is only 4 %, rather than 4.6 % when the new branch is not accounted for.

We find the change in radiative forcing due to changes in O_3 since pre-industrial

times to be $0.26\,\mathrm{W\,m^{-2}}$ with the new branch, compared to $0.33\,\mathrm{W\,m^{-2}}$ without. This decrease is due to changes in tropospheric O$_3$ shifting the RF from 0.45 to $0.38\,\mathrm{W\,m^{-2}}$, while the RF due to stratospheric O$_3$ changes is unchanged at $-0.12\,\mathrm{W\,m^{-2}}$. Overall, we find from our results that RF due to changes in tropospheric and stratospheric O$_3$

5   is quite different from the RF due to O$_3$ change from tropospheric and stratospheric O$_3$ precursors.

The inclusion of the new reaction branch substantially improved the agreement of the modelled tropical upper tropospheric O$_3$ with sonde measurements, and also for the aircraft measurement comparison. The new branch also improved the agreement

10 between modelled global mean OH concentrations and recent estimates. We find it not possible to conclude whether NO and NO$_y$ are improved or not.

It was found by Butkovskaya et al. (2005), that taking the abundance of water vapour into account increases the branching ratio in the direction of HNO$_3$ formation, however as yet there is no parameterisation of this effect which would be suitable for incorpora-

15 tion into an atmospheric model. If such a parameterisation were to become available in the future, this study should be revisited.

The results of this work, however, already show that the existence of a HNO$_3$ forming branch of the HO$_2$ + NO reaction has very important implications both for the modelling of present day atmospheric composition, as well as for assessing the anthropogenic

20 impact on the atmosphere since pre-industrial times, and therefore the branching ratios and rates of this reaction should be confirmed by other laboratory studies.

References

Berglen, T. F., Berntsen, T. K., Isaksen, I. S. A., and Sundet, J. K.: A global model of the coupled sulfur/oxidant chemistry in the troposphere: the sulfur cycle, J. Geophys. Res., 109, D19310, doi:10.1029/2003JD003948, 2004. 14805

Berntsen, T. and Isaksen, I. S. A.: A global 3-D chemical transport model for the troposphere. 1. Model description and CO and ozone results, J. Geophys. Res., 102, 21239–21280, doi:10.1029/97JD01140, 1997. 14805

Berntsen, T., Isaksen, I., Myhre, G., Fuglestvedt, J., Stordal, F., Larsen, T., Freckleton, R., and Shine, K.: Effects of anthropogenic emissions on tropospheric ozone and its radiative forcing, J. Geophys. Res., 102, 28101–28126, doi:10.1029/97JD02226, 1997. 14803, 14817

Berntsen, T. K. and Isaksen, I. S. A.: Effects of lightning and convection on changes in upper tropospheric ozone due to NO_x emissions from aircraft, Tellus B, 51, 766–788, doi:10.1034/j.1600-0889.1999.t01-3-00003.x, 1999. 14806

Brenninkmeijer, C. A. M., Crutzen, P., Boumard, F., Dauer, T., Dix, B., Ebinghaus, R., Filippi, D., Fischer, H., Franke, H., Frieß, U., Heintzenberg, J., Helleis, F., Hermann, M., Kock, H. H., Koeppel, C., Lelieveld, J., Leuenberger, M., Martinsson, B. G., Miemczyk, S., Moret, H. P., Nguyen, H. N., Nyfeler, P., Oram, D., O'Sullivan, D., Penkett, S., Platt, U., Pupek, M., Ramonet, M., Randa, B., Reichelt, M., Rhee, T. S., Rohwer, J., Rosenfeld, K., Scharffe, D., Schlager, H., Schumann, U., Slemr, F., Sprung, D., Stock, P., Thaler, R., Valentino, F., van Velthoven, P., Waibel, A., Wandel, A., Waschitschek, K., Wiedensohler, A., Xueref-Remy, I., Zahn, A., Zech, U., and Ziereis, H.: Civil Aircraft for the regular investigation of the atmosphere based on an instrumented container: The new CARIBIC system, Atmos. Chem. Phys., 7, 4953–4976, doi:10.5194/acp-7-4953-2007, 2007. 14813

Butkovskaya, N., Kukui, A., Pouvesle, N., and Le Bras, G.: Formation of nitric acid in the gasphase $HO_2 + NO$ reaction: effects of temperature and water vapor, J. Phys. Chem. A, 109, 6509–6520, doi:10.1021/jp051534v, 2005. 14803, 14804, 14818

Butkovskaya, N., Kukui, A., and Le Bras, G.: HNO_3 forming channel of the $HO_2 + NO$ reaction as a function of pressure and temperature in the ranges of 72–600 Torr and 223–323 K, J. Phys. Chem. A, 111, 9047–9053, doi:10.1021/jp074117m, 2007. 14804

Cariolle, D., Evans, M. J., Chipperfield, M. P., Butkovskaya, N., Kukui, A., and Le Bras, G.: Impact of the new HNO_3-forming channel of the $HO_2 + NO$ reaction on tropospheric HNO_3, NO_x, HO_x and ozone, Atmos. Chem. Phys., 8, 4061–4068, doi:10.5194/acp-8-4061-2008,

Title Page

Abstract | Introduction

Conclusions | References

Tables | Figures

◄◄ | ►►

◄ | ►

Back | Close

Full Screen / Esc

Printer-friendly Version

Interactive Discussion

2008. 14804, 14807, 14809, 14814, 14815

Chen, C., Shepler, B. C., Braams, B. J., and Bowman, J. M.: Quasiclassical trajectory calculations of the $HO_2 + NO$ reaction on a global potential energy surface, Phys. Chem. Chem. Phys., 11, 4722–4727, doi:10.1039/b823031e, 2009. 14804

5 Forster, P., Ramaswamy, V., Artaxo, P., Berntsen, T., Betts, R., Fahey, D., Haywood, J., Lean, J., Lowe, D., Myhre, G., Nganga, J., Prinn, R., Raga, G., Schulz, M., and Van Dorland, R.: Climate Change 2007: The Physical Science Basis. Contribution of Working Group I to the Fourth Assessment Report of the Intergovernmental Panel on Climate Change, chap. 2, Changes in Atmospheric Constituents and in Radiative Forcing, Cambridge University Press,
10 Cambridge, UK and New York, NY, USA, 2007. 14815

Gauss, M., Myhre, G., Isaksen, I. S. A., Grewe, V., Pitari, G., Wild, O., Collins, W. J., Dentener, F. J., Ellingsen, K., Gohar, L. K., Hauglustaine, D. A., Iachetti, D., Lamarque, F., Mancini, E., Mickley, L. J., Prather, M. J., Pyle, J. A., Sanderson, M. G., Shine, K. P., Stevenson, D. S., Sudo, K., Szopa, S., and Zeng, G.: Radiative forcing since preindustrial times
15 due to ozone change in the troposphere and the lower stratosphere, Atmos. Chem. Phys., 6, 575–599, doi:10.5194/acp-6-575-2006, 2006. 14803

Granier, C., Lamarque, J. F., Mieville, A., Muller, J. F., Olivier, J., Orlando, J., Peters, J., Petron, G., Tyndall, G., and Wallens, S.: POET, a database of surface emissions of ozone precursors, available at: http://www.aero.jussieu.fr/projet/ACCENT/POET.php, 2005. 14806

20 Hauglustaine, D. A. and Brasseur, G. P.: Evolution of tropospheric ozone under anthropogenic activities and associated radiative forcing of climate, J. Geophys. Res., 106, 32337–32360, doi:10.1029/2001JD900175, 2001. 14803

Hesstvedt, E., Hov, O., and Isaksen, I. S. A.: Quasi steady-state approximation in air pollution modelling: comparison of two numerical schemes for oxidant prediction, Int. J. Chem. Kinet.,
25 X, 971–994, doi:10.1002/kin.550100907, 1978. 14806

Holtslag, A. A. M., DeBruijn, E. I. F., and Pan, H.-L.: A high resolution air mass transformation model for short-range weather forecasting, Mon. Weather Rev., 118, 1561–1575, doi:10.1175/1520-0493(1990)118<1561:AHRAMT>2.0.CO;2, 1990. 14805

IPCC: Climate Change 2001: The Scientific Basis. Contribution of Working Group I to the
30 Third Assessment Report of the Intergovernmental Panel on Climate Change, Cambridge University Press, Cambridge, UK and New York, NY, USA, 881 pp., 2001. 14803

IPCC AR4: Climate Change 2007: The Physical Science Basis. Contribution of Working Group I to the Fourth Assessment Report of the Intergovernmental Panel on Climate Change, Cam-

bridge University Press, Cambridge, United Kingdom and New York, NY, USA, 996 pp., 2007. 14803

Isaksen, I. S. A., Zerefos, C., Kourtidis, K., Meleti, C., Dalsøren, S. B., Sundet, J. K., Grini, A., Zanis, P., and Balis, D.: Tropospheric ozone changes at unpolluted and semipolluted regions induced by stratospheric ozone changes, J. Geophys. Res., 110, D02302, doi:10.1029/2004JD004618, 2005. 14805

Lamarque, J. F., Hess, P., Emmons, L., Buja, L., Washington, W., and Granier, C.: Tropospheric ozone evolution between 1890 and 1990, J. Geophys. Res., 110, D08304, doi:10.1029/2004JD005537, 2005. 14803

Myhre, G. and Stordal, F.: Role of spatial and temporal variations in the computation of radiative forcing and GWP, J. Geophys. Res., 102, 11181–11200, doi:10.1029/97JD00148, 1997. 14815

Myhre, G., Karlsdóttir, S., Isaksen, I., and Stordal, F.: Radiative forcing due to changes in tropospheric ozone in the period 1980 to 1996, J. Geophys. Res., 105, 28935–28942, doi:10.1029/2000JD900187, 2000. 14815

Olivier, J., Peters, J., Granier, C., Petron, G., Müller, J. F., and Wallens, S.: Present and future emissions of atmospheric compounds, POET report #2, EU report EV K2-1999-00011, 2003. 14806

Prather, M. J.: Numerical advection by conservation of second-order moments, J. Geophys. Res., 91, 6671–6681, doi:10.1029/JD091iD06p06671, 1986. 14805

Price, C. and Rind, D.: What determines the cloud-to-ground lightning fraction in thunderstorms, Geophys. Res. Lett., 20, 463–466, doi:10.1029/93GL00226, 1993. 14806

Shindell, D. T., Faluvegi, G., and Bell, N.: Preindustrial-to-present-day radiative forcing by tropospheric ozone from improved simulations with the GISS chemistry-climate GCM, Atmos. Chem. Phys., 3, 1675–1702, doi:10.5194/acp-3-1675-2003, 2003. 14803

Schumann, U. and Huntrieser, H.: The global lightning-induced nitrogen oxides source, Atmos. Chem. Phys., 7, 3823–3907, doi:10.5194/acp-7-3823-2007, 2007. 14815

Søvde, O. A., Gauss, M., Smyshlyaev, S. P., and Isaksen, I. S. A.: Evaluation of the chemical transport model Oslo CTM2 with focus on Arctic winter ozone depletion, J. Geophys. Res., 113, doi:10.1029/2007jd009240, 2008. 14804, 14805, 14806, 14807

Søvde, O. A., Orsolini, Y. J., Jackson, D. R., Stordal, F., Isaksen, I. S. A., and Rognerud, B.: Estimation of Arctic O_3 loss during winter 2006/2007 using data assimilation and comparison with a chemical transport model, Q. J. Roy. Meteorol. Soc., 137, 118–128,

Title Page

Abstract | Introduction

Conclusions | References

Tables | Figures

◄ | ►

◄ | ►

Back | Close

Full Screen / Esc

Printer-friendly Version

Interactive Discussion

doi:10.1002/qj.740, 2011. 14805

Stamnes, K., Tsay, S., Wiscombe, W., and Jayaweera, K.: Numerically stable algorithm for discrete-ordinate-method radiative transfer in multiple scattering and emitting layered media, Appl. Opt., 27, 2502–2509, doi:10.1364/AO.27.002502, 1988. 14815

5 Thompson, A. M., Witte, J., McPeters, R., Oltmans, S., Schmidlin, F., Logan, J., Fujiwara, M., Kirchhoff, V., Posny, F., Coetzee, G., Hoegger, B., Kawakami, S., Ogawa, T., Johnson, B., Vömel, H., and Labow, G.: Southern Hemisphere Additional Ozonesondes (SHADOZ) 1998–2000 tropical ozone climatology. 1. Comparison with Total Ozone Mapping Spectrometer (TOMS) and ground-based measurements, J. Geophys. Res., 108, 8238,

10 doi:10.1029/2001JD000967, 2003. 14812

Wang, J. S., McElroy, M. B., Logan, J. A., Palmer, P. I., Chameides, W. L., Wang, Y., and Megretskaia, I. A.: A quantitative assessment of uncertainties affecting estimates of global mean OH derived from methyl chloroform observations, J. Geophys. Res., 113, D12302, doi:10.1029/2007JD008496, 2008. 14809

15 WMO: Scientific assessment of ozone depletion: 2006., World Meteorological Organization: Global Ozone Research and Monitoring Project – Report No. 50, World Meteorological Organization, Geneva, Switzerland, 2007. 14806

Wong, S., Wang, W.-C., Isaksen, I. S. A., Berntsen, T. K., and Sundet, J. K.: A global climate-chemistry model study of present-day tropospheric chemistry and radiative forcing from

20 changes in tropospheric O_3 since the preindustrial period, J. Geophys. Res., 109, D11309, doi:10.1029/2003JD003998, 2004. 14803

Title Page

Abstract | Introduction

Conclusions | References

Tables | Figures

◄ | ►|

◄ | ►

Back | Close

Full Screen / Esc

Printer-friendly Version

Interactive Discussion

Table 1. The model runs carried out in this study.

Model run	Description
REF_2000	Present day reference run, without Eq. (2)
REF_1850	Pre-industrial reference run, without Eq. (2)
R2_2000	Present day run, Eq. (2) included
R2_1850	Pre-industrial run, Eq. (2) included

Title Page

Abstract | Introduction

Conclusions | References

Tables | Figures

◄◄ | ►►

◄ | ►

Back | Close

Full Screen / Esc

Printer-friendly Version

Interactive Discussion

Table 2. The tropospheric, annual mean OH concentration (10^6 molec cm^{-3}), for each of the model runs. The difference (Δ) between the R2 and REF runs is given in brackets. The last column shows the difference between the OH concentration in 2000 and 1850 for each run, with the effect of R2 on this change given in brackets.

Model run	[OH], (Δ from REF_2000) 1850	2000	Δ
REF	1.52	1.35	-11.2%
R2	1.32 (-13.2%)	1.16 (-14.1%)	-12.1% (8.0%)

O. A. Søvde et al.

Table 3. As for Table 2, except for tropospheric, annual mean CH$_4$ lifetime τ_{CH_4}.

Model run	τ_{CH_4} (years), (Δ from REF_2000) 1850	2000	Δ
REF	6.71	7.02	4.6 %
R2	7.44 (10.3 %)	7.74 (10.9 %)	4.0 % (−13.0 %)

Table 4. Locations of SHADOZ stations used for the mean profile in Fig. 6. #prof is the number of profiles used in mean values.

Name	longitude (° E)	latitude (° N)	#prof.
American Samoa	189.44	−14.23	40
Ascension	345.58	−7.98	31
Fiji	178.40	−18.13	38
Irene	28.22	−25.90	40
Java, Watukosek	112.65	−7.57	44
Kuala Lumpur	101.70	2.73	25
La Réunion	55.48	−21.06	37
Nairobi	36.80	1.27	39
Natal	324.62	−5.42	34
Paramaribo	304.79	5.81	48
San Cristóbal	270.40	−0.92	56
Total			432

Table 5. The different components of the radiative forcing due to the change in O_3 since the pre-industrial times.

RF due to tropospheric O_3 change		
Component	REF	R2
Tropospheric O_3 precursors	0.50	0.44
Cl & Br	−0.05	−0.06
Total RF, trop.	0.45	0.38
RF due to stratospheric O_3 change		
Component	REF	R2
Tropospheric O_3 precursors	0.09	0.08
Cl & Br	−0.21	−0.20
Total RF, strat.	−0.12	−0.12
RF due to tropospheric & stratospheric O_3 change		
Component	REF	R2
Tropospheric O_3 precursors	0.59	0.52
Cl & Br	−0.26	−0.26
Total RF, trop. & strat.	0.33	0.26
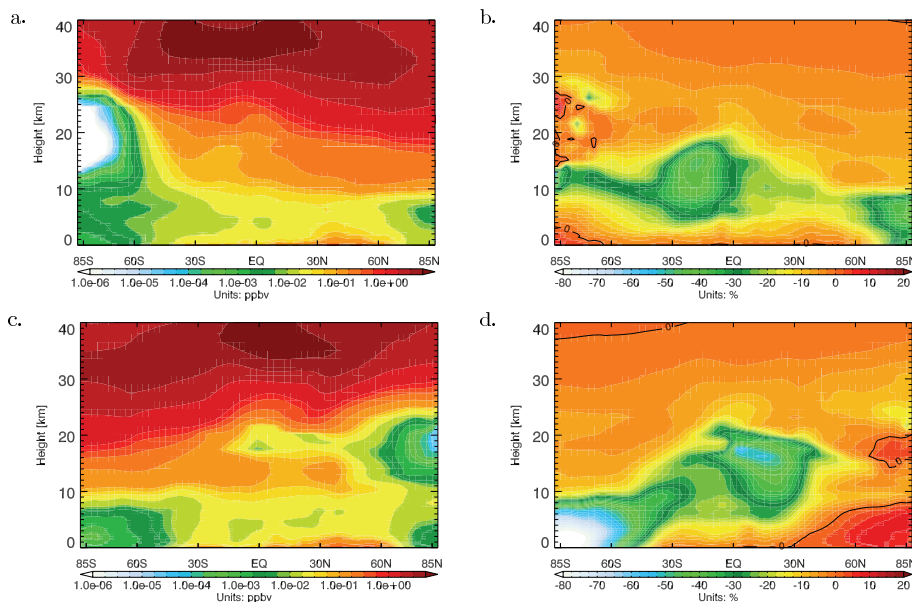
Fig. 1. The zonal mean NO$_2$ mixing ratio in REF_2000, for July **(a)** and December **(c)**. Panels **(b)** and **(d)** show the percent change in mixing ratio from REF_2000 to R2_2000, for July and December, respectively.
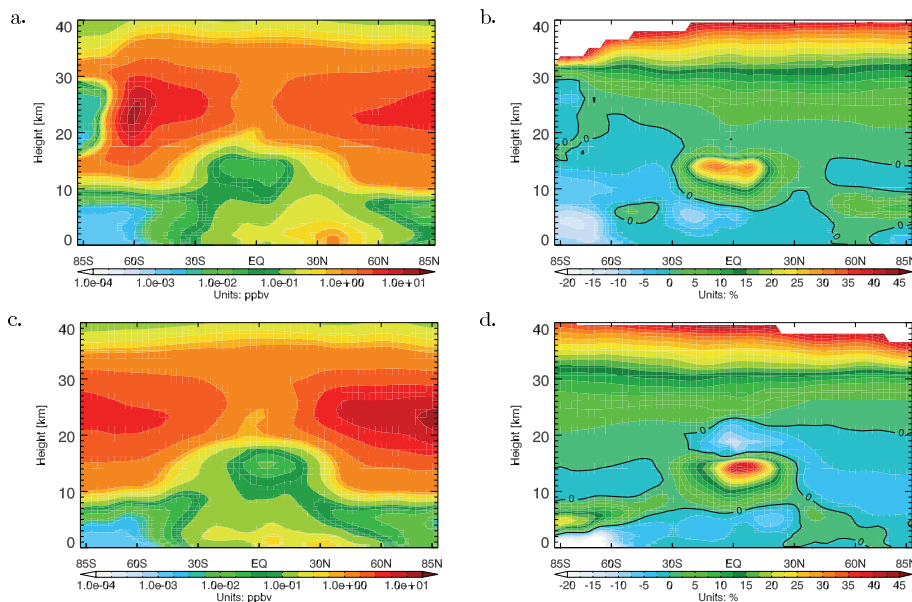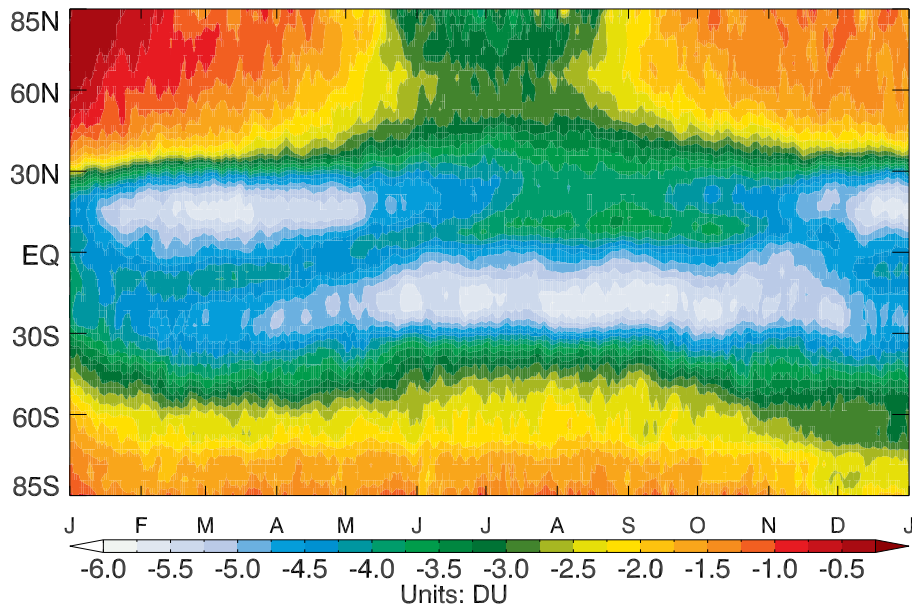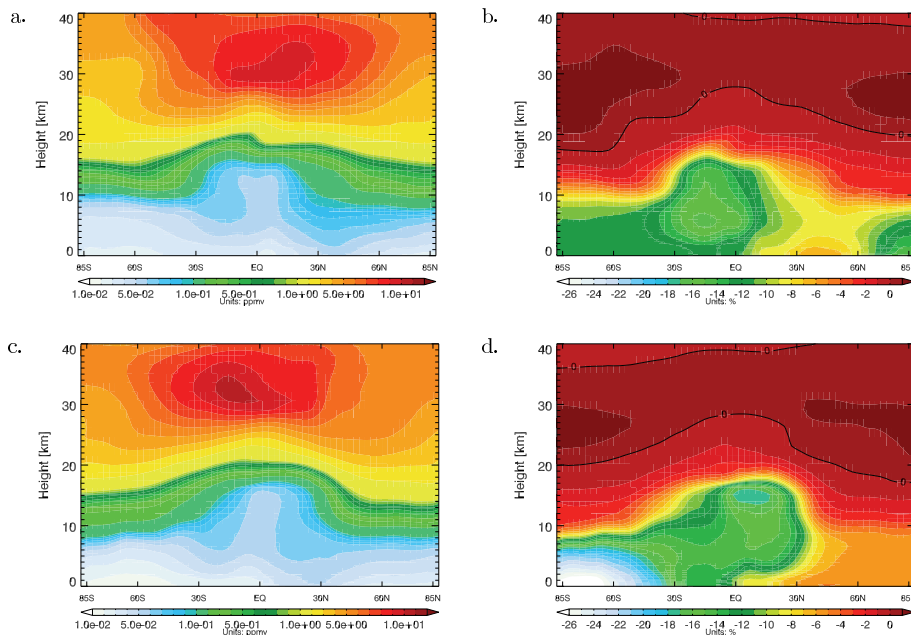
Fig. 2. The zonal mean HNO$_3$ mixing ratio in REF_2000, for July **(a)** and December **(c)**. Panels **(b)** and **(d)** show the percent change in mixing ratio from REF_2000 to R2_2000, for July and December, respectively.

Full Screen / Esc

Fig. 3. The change in zonal, tropospheric mean modelled O$_3$ column, between REF_2000 and R2_2000, as a function of time.

O. A. Søvde et al.

Title Page

Abstract	Introduction
Conclusions	References
Tables	Figures

⏮ | ▶�|

◀ | ▶

Back | Close

Full Screen / Esc

Printer-friendly Version

Interactive Discussion

Fig. 4. The zonal mean O_3 mixing ratio in REF_2000, for July **(a)** and December **(c)**. Panels **(b)** and **(d)** show the percent change in mixing ratio from REF_2000 to R2_2000, for July and December, respectively.
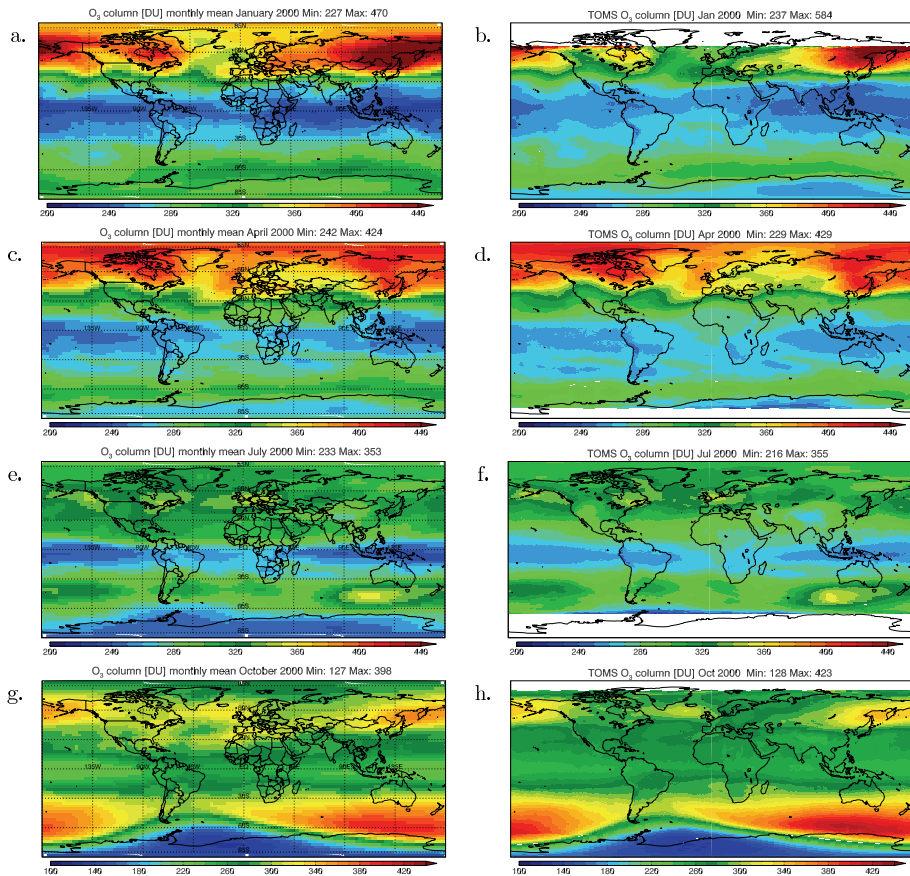
Fig. 5. The zonal, monthly mean mixing ratio of O_3 from run R2_2000, for July 2000. Note the different scale in October.

ACPD

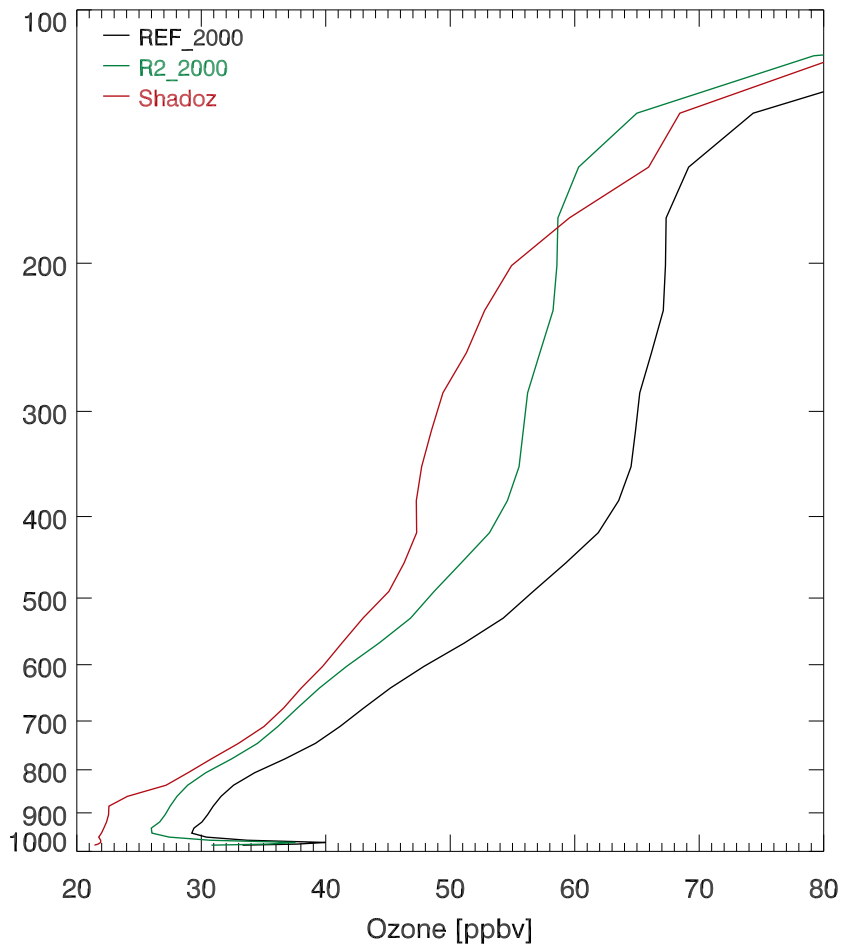11, 14801–14835, 2011

$HO_2 + NO \rightarrow HNO_3$

O. A. Søvde et al.

Title Page

Abstract | Introduction

Conclusions | References

Tables | Figures

◄ | ►

Back | Close

Full Screen / Esc

Printer-friendly Version

Interactive Discussion

Fig. 6. A comparison of annual mean profiles from SHADOZ, with corresponding profiles from REF_2000 and R2_2000.
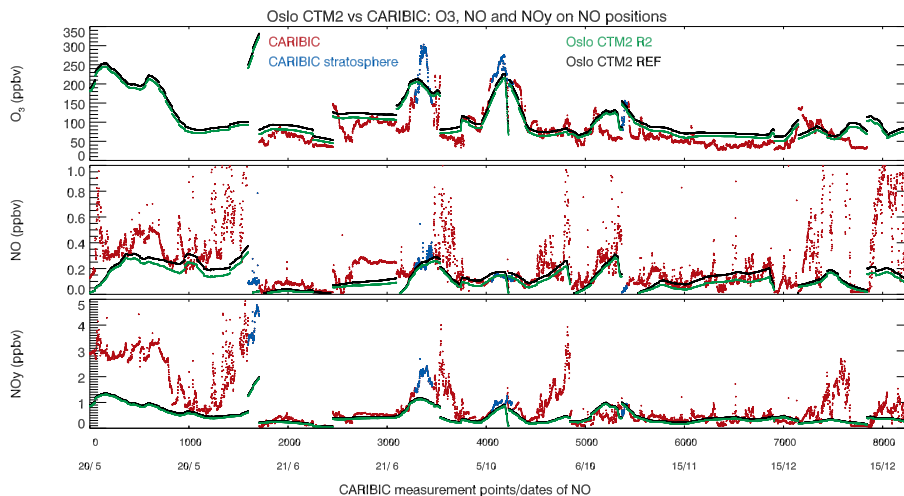
Fig. 7. A comparison of Oslo CTM2 on CARIBIC flight routes for 2005, on all measurement locations/times where NO was measured above 400 hPa. Blue dots are measurements above the tropopause, as defined by the Oslo CTM2. Model results are produced at the same time and location as aircraft measurements.

Discussion Paper | Discussion Paper | Discussion Paper | Discussion Paper | Discussion Paper |

Title Page

Abstract | Introduction

Conclusions | References

Tables | Figures

|◄ | ►|

◄ | ►

Back | Close

Full Screen / Esc

Printer-friendly Version

Interactive Discussion
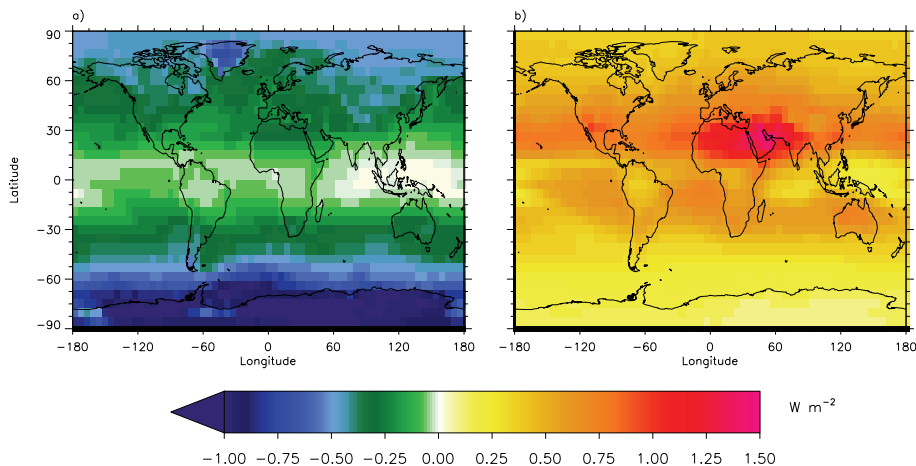
Fig. 8. The radiative forcing due to changes in atmospheric O$_3$ between the pre-industrial times and the present, for the R2 simulations. **(a)** shows the RF for the change in stratospheric O$_3$, **(b)** the RF for the change in tropospheric O$_3$.